


# Lanthionine Ketimine Ethyl Ester Accelerates Remyelination in a Mouse Model of Multiple Sclerosis

ASN Neuro  
Volume 14: 1–15  
© The Author(s) 2022  
Article reuse guidelines:  
sagepub.com/journals-permissions  
DOI: 10.1177/17590914221112352  
journals.sagepub.com/home/asn



Jeffrey L. Dupree<sup>1,2</sup>, Pablo M. Paez<sup>3</sup> ,  
Seema K. Tiwari-Woodruff<sup>4</sup> , Travis T. Denton<sup>5,6,7</sup>,  
Kenneth Hensley<sup>8</sup>, Christina G. Angeliu<sup>3</sup>, Anne I. Boullerne<sup>9</sup>,  
Sergey Kalinin<sup>9</sup>, Sophia Egge<sup>1</sup>, Veronica T. Cheli<sup>3</sup>,  
Giancarlo Denaroso<sup>3</sup>, Kelley C. Atkinson<sup>4</sup>, Micah Feri<sup>4</sup>  
and Douglas L. Feinstein<sup>9,10</sup> 

## Abstract

Although over 20 disease modifying therapies are approved to treat Multiple Sclerosis (MS), these do not increase remyelination of demyelinated axons or mitigate axon damage. Previous studies showed that lanthionine ketimine ethyl ester (LKE) reduces clinical signs in the experimental autoimmune encephalomyelitis (EAE) mouse model of MS and increased maturation of oligodendrocyte (OL) progenitor cells (OPCs) *in vitro*. In the current study, we used the cuprizone (CPZ) demyelination model of MS to test if LKE could increase remyelination. The corpus callosum (CC) and somatosensory cortex was examined by immunohistochemistry (IHC), electron microscopy and for mRNA expression changes in mice provided 5 weeks of CPZ diet followed by 2 weeks of normal diet in the presence of LKE or vehicle. A significant increase in the number of myelinated axons, and increased myelin thickness was observed in the CC of LKE-treated groups compared to vehicle-treated groups. LKE also increased myelin basic protein and proteolipid protein expression in the CC and cortex, and increased the number of mature OLs in the cortex. In contrast, LKE did not increase the percentage of proliferating OPCs suggesting effects on OPC survival and differentiation but not proliferation. The effects of LKE on OL maturation and remyelination were supported by similar changes in their relative mRNA levels. Interestingly, LKE did not have significant effects on GFAP or Iba1 immunostaining or mRNA levels. These findings suggest that remyelinating actions of LKE can potentially be formulated to induce remyelination in neurological diseases associated with demyelination including MS.

## Keywords

myelination < NEURO development, oligodendrocytes < NEURO glia, regeneration < NEURO repair, demyelination < NEURO degeneration

<sup>1</sup>Department of Anatomy and Neurobiology, Virginia Commonwealth University, Richmond, VA, USA

<sup>2</sup>Research Service, HH McGuire VA Medical Center, Richmond, VA, USA

<sup>3</sup>Institute for Myelin and Glia Exploration, Department of Pharmacology and Toxicology, University at Buffalo, NY, USA

<sup>4</sup>Division of Biomedical Sciences, School of Medicine at the University of California Riverside, Riverside, CA, USA

<sup>5</sup>Department of Pharmaceutical Sciences, College of Pharmacy & Pharmaceutical Sciences, Washington State University Health Sciences Spokane, Spokane, WA, USA

<sup>6</sup>Department of Translational Medicine and Physiology, Elson S. Floyd College of Medicine, Washington State University Health Sciences Spokane, Spokane, WA, USA

<sup>7</sup>Steve Gleason Institute for Neuroscience, Washington State University Health Sciences Spokane, Spokane, WA, USA

<sup>8</sup>Arkansas College of Osteopathic Medicine, Fort Smith, AR, USA

<sup>9</sup>Department Anesthesiology, University of Illinois, Chicago, IL, USA

<sup>10</sup>Jesse Brown VA Medical Center, Chicago, IL, USA

\*Equal contributors

## Corresponding Author:

Douglas L. Feinstein, Department of Anesthesiology, University of Illinois, 835 South Wolcott Avenue, MC 513, Chicago IL, 60612, USA.

Email: dlfeins@uic.edu



Received October 28, 2021; Revised June 17, 2022; Accepted for publication June 21, 2022

## Introduction

Multiple sclerosis (MS) is the most common neurodegenerative disease in young adults affecting close to 1 million MS patients in the USA (Wallin et al., 2019) and over 2 million people world-wide. The main hallmark of MS is the presence of disseminated demyelinated lesions in both white as well as grey matter of the central nervous system (CNS) including the brain stem, spinal cord, and optic nerve (Reich et al., 2018; Thompson et al., 2018). In some cases, remyelination occurs, and ‘shadow plaques’, areas containing axons with thinner myelin sheaths, can be observed which represent areas in which all axons have been remyelinated. However, in the majority of cases remyelination is limited, associated with loss of mature oligodendrocytes (OLGs), and reduced capacity of immature OLG progenitor cells (OPCs) to differentiate to a myelinating phenotype or achieve successful myelination (Chang et al., 2002). Demyelination leads to reductions in nerve conduction with motor, sensory, and cognitive or behavioral deficits, and results in neuronal damage and loss. Thus, developing treatments to promote remyelination should reduce irreversible neuronal damage and loss. There are currently over 20 FDA approved drugs to treat MS, however, these primarily target adaptive immune responses and none significantly influence remyelination or stop disease progression in progressive forms of MS.

Lanthionine is a non-proteogenic amino acid synthesized via trans-sulfuration of cysteine with serine or a 2<sup>nd</sup> cysteine by cystathionine  $\beta$ -synthase (Hensley et al., 2010a; Hensley & Denton, 2015). Lanthionine is a substrate for the enzyme glutamine transaminase K which yields an intermediate that cyclizes to form lanthionine ketenamine (LK). LK can be further derivatized to yield the ethyl ester LKE which has increased cellular permeability (Shen et al., 2018). LKE promotes elongation and thickening of neurites, suppresses microglial nitric oxide production, and protects motor neurons from microglial-induced toxicity (Hensley et al., 2013; Hubbard et al., 2013; Nada et al., 2012). LKE is an orally bioavailable, brain-penetrating, non-toxic, small molecule that shows beneficial effects in mouse models of neurodegenerative diseases and conditions including Alzheimer’s disease (Hensley et al., 2013; Koehler et al., 2018), ischemia (Nada et al., 2012), and amyotrophic lateral sclerosis (Khanna et al., 2012); improves neurological outcome after fluid percussion injury (Hensley et al., 2016), and promotes locomotor recovery after spinal cord injury (Kotaka et al., 2017).

These properties led to testing of LKE for beneficial actions in the myelin oligodendrocyte glycoprotein (MOG) 35–55 peptide induced chronic experimental autoimmune

encephalomyelitis (EAE) mouse model of MS. Treatment with LKE reduced clinical scores, glial inflammation and axonal damage, and showed a trend towards increasing myelin thickness (Dupree et al., 2015). Subsequently, the effects of LKE were tested using primary rat OPCs and showed that LKE increases OPC process number and length, (Savchenko et al., 2019) associated with increased expression of several myelin genes. In other studies, LKE was shown to reduce excitotoxicity and increase neuronal process numbers and length in human SH-SY5Y cells and mouse cerebellar granule cells (Marangoni et al., 2018) suggesting effects on neuronal survival and maturation. However, whether some or all of these actions account for the beneficial effects of LKE in EAE is not known. To begin to address this, we examined the effects of LKE on the remyelination phase that occurs in the cuprizone (CPZ) induced, non-inflammatory demyelinating mouse model. We find that, compared to the remyelination that occurs when mice are given control chow, after 2 weeks recovery mice provided chow supplemented with LKE show increased myelin thickness, reduced axonal swelling, almost complete restoration of normal g-ratios, and an increase in the percentage of remyelinated axons. LKE also increased the number of Olig2+ and CC1+ OLGs without change in the number of proliferating OLGs, suggesting its effects on remyelination involve increased survival or maturation of OPCs.

## Methods and Materials

### Materials

LKE was synthesized as described (Hensley et al., 2010a) with minor modifications. In brief, a solution of ethyl cysteine hydrochloride (1.48 g, 8.01 mmol) in water (8 mL) was added to a stirring solution of bromopyruvate (1.56 g, 8.41 mmol) in water (10 mL) over 30 s. After about 1 min, a solid began to form. The flask was purged with Argon gas, then stirred overnight (ca. 18 h), then the white solid was collected from the brownish slurry by vacuum filtration (Buchner funnel, #4 filter paper), and the residual volatiles were removed under high vacuum. LKE (1.36 g, 78.24% yield) was recovered as a white solid, and determined to be >99% pure by <sup>1</sup>H NMR analysis.

### Cuprizone Treatment

Female C57BL/6 mice aged 7 to 8 weeks were purchased from Envigo (Madison, WI, USA). Cortical demyelination and remyelination was carried out as described (Clark et al., 2016).

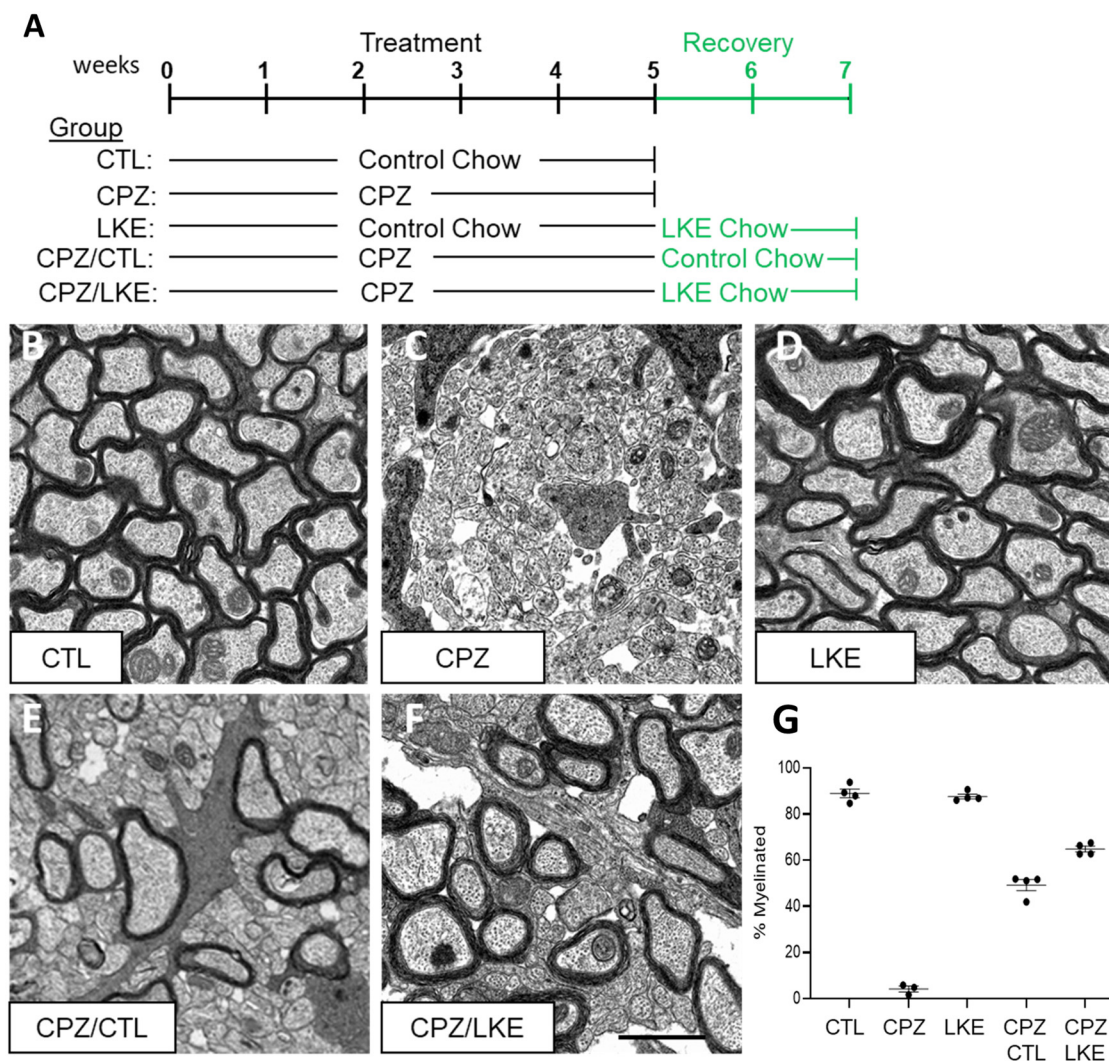


**Figure 1.** LKE increases the percentage of myelinated axons. (A) Overview of experimental protocol. Mice were kept on control chow (CTL) or chow containing CPZ (CPZ) for 5 weeks. LKE mice were kept on control chow for 5 weeks then provided chow containing 100 ppm LKE for a further 2 weeks. CPZ/CTL and CPZ/LKE mice were kept on CPZ containing chow for 5 weeks then switched to control or LKE containing chow for a further 2 weeks. (B–F) Representative EM images of sections from the corpus callosum from each of the 5 experimental groups. Size bar is 2 microns. (G) The percentage of myelinated axons. Data is mean  $\pm$  SE, n = 3 (CPZ) or n = 4 (all other groups) mice per group, an average of 11 images per mouse, and an average of 75 axons per image, for an average total # of axons counted per mouse of 860 (control), 635 (CPZ), 911 (LKE), 908 (CPZ/CTL), and 641 (CPZ/LKE). 1-way ANOVA  $F = 152.1$ ,  $P < 0.0001$ . All groups were significantly different from all other groups ( $P < 0.0001$ ) by Tukey's multiple comparison tests except for CTL versus LKE (not significant).

Ground rodent chow (5001 Rodent Diet; PMI Nutrition International, LLC, Brentwood, MO) was mixed with cuprizone (CPZ, Bis(cyclohexanone) oxaldihydrazone; Sigma-Aldrich, St. Louis, MO). Nine-week-old female C57BL/6 mice were divided into 5 groups (Figure 1). Mice were provided normal chow; or chow with 0.2% w/w CPZ. After 5 weeks, control (CTL) and CPZ (CPZ) mice were sacrificed. The remaining CPZ-treated mice were placed back onto normal chow (CPZ/CTL) or normal chow supplemented with 100 ppm LKE (CPZ/LKE). A second control group (LKE) were mice given control chow for 5 weeks then chow supplemented with 100 ppm LKE. After 2 weeks, mice were sacrificed. All mice

were transcardially perfused with 4% paraformaldehyde in PBS, brains dissected, one hemisphere processed for electron microscopic analysis and the other hemisphere used for immunohistochemical analysis. All animal procedures were conducted using humane conditions, and were approved by the McGuire Institutional Animal Care and Use Committee protocols 1661570 and 1573009.

### Electron Microscopy Analysis

Mice were prepared for transmission electron microscopic analysis as described (Dupree & Feinstein, 2018). Following

dissection, one hemisphere from each mouse was post fixed in 1 M Millonig's buffer containing 4% paraformaldehyde and 5% glutaraldehyde. Following 2 weeks of aldehyde post-fixation, hemispheres were rinsed in 0.1 M cacodylate buffer, post-fixed in 2% osmium tetroxide, rinsed in 0.1 M cacodylate buffer, dehydrated in serial dilutions of ethanol, and embedded in PolyBed 812 resin (PolySciences, Warrington, PA, USA). Ultrathin (70 nm) sections containing the caudal third of the corpus callosum (CC) were stained with uranyl acetate and lead citrate and imaged using a JEOL JEM 1400Plus transmission electron microscope (JEOL, Peabody, MA, USA) equipped with a Gatan OneView CMOS camera (Gatan Inc., Pleasanton, CA, USA). A minimum of 115 myelinated axons per mouse from electron micrographs (10,000x magnification) collected from the CC at the level of the fornix (between 0.7 and 1.06 mm posterior to Bregma) were quantitatively analyzed to determine axon caliber, myelin thickness, and calculate g-ratios. Image analysis was done by an observer blinded to the experimental groups.

### Immunohistochemistry

Following perfusion in 4% paraformaldehyde in PBS, hemispheres were post-fixed overnight in 1 M Millonig's buffer containing 4% paraformaldehyde and 5% glutaraldehyde at 4°C. Coronal brain slices 50µm thick were obtained using a vibratome (Leica Biosystems, VT1000-S). Free-floating sections were incubated in blocking solution (2% normal goat serum and 1% Triton X-100 in PBS) for 2 h at room temperature, then incubated with primary antibodies overnight at 4°C. Sections were then rinsed in PBS and incubated with Cy3 or Cy5 conjugated secondary antibodies (1:400; Jackson Immuno Research) for 2 h at room temperature followed by a counterstain with the nuclear dye DAPI (Life Technologies). After washing, sections were mounted onto Superfrost Plus slides (Fisher) using coverslips and mounting medium (Aquamount; Thermo Scientific). The staining intensity and the number of positively stained cells was assessed in the central area of the CC, between the midline and below the apex of the cingulum (0.6mm<sup>2</sup>) (Franklin & Paxinos, 2008). The integrated fluorescence intensity for both the CC and the overlying somatosensory cortex (CX) was calculated as the product of the area and mean pixel intensity using MetaMorph software (Molecular Devices, RRID: SCR\_002368). For all experiments involving quantification of positive cells and fluorescent intensity, data represent pooled results from at least 3 brains per experimental group. At least 10 slices per brain (50µm each) were used and quantification was performed using an unbiased stereological sampling method. The image analysis was done by an observer blinded to the experimental groups. The primary antibodies used were against: CC1 (mouse; 1:300; Calbiochem, RRID: AB\_2057371), Ki67 (rabbit; 1:250; Abcam, RRID: AB\_443209), MBP (mouse; 1:1000; Covance, RRID: AB\_510039), Olig2 (mouse and rabbit; 1:500; Millipore,

RRID: AB\_570666, RRID: AB\_10807410), PLP (rat; 1:500, AA3 – PLP/DM20, RRID: AB\_2341144), GFAP (rabbit, 1:1000; Dako), and Iba1 (rabbit, 1:800; Wako, RRID: AB\_839504). Since there were no differences observed between the LKE and the CTL groups, representative images are not included for LKE, although the quantitative analysis is provided.

### RNA Quantitation

RNA was isolated from tissue samples containing CC and overlying CX, using Direct-zol RNA MicroPrep (Zymo Research) according to instructions. Total RNA (1 µg) was converted to cDNA using the High-Capacity cDNA Reverse Transcription Kit (ThermoFisher 4368814). The cDNA was amplified with specific primers (Table S1) using FastStart Universal SYBR Green Master mix (Applied Biosystems, 04913914001) in a BioRad CFX96 real time PCR machine (BioRad, Hercules, CA). Relative mRNA levels were calculated from threshold take-off cycle number and normalized to values measured for β-actin in the same samples.

### Data Analysis

Group averages were compared by ordinary 1-way ANOVA, and frequency distributions compared by 2-way ANOVA, both with Tukey's multiple comparison post hoc tests. Outliers were identified using Grubb's method. Significant differences between all groups are presented, except for comparisons to the LKE group which never differed from the CTL group. Comparisons were made using GraphPad Prism 9.2 and significance assumed at  $P < 0.05$ .

### Results

In the CPZ model, significant and robust remyelination occurs during the recovery period after CPZ is removed from the diet, commencing as soon 1 week after withdrawal, and continuing over the next 6 weeks (Skripuletz et al., 2008; Stidworthy et al., 2003). To examine the effects of LKE during the early stages of remyelination, we compared sections through the CC prepared 2 weeks after recovery on normal chow to recovery on chow containing LKE. In control mice without CPZ treatment, close to 90% of the axons in the CC were myelinated (Figure 1G); while after 5 weeks treatment with CPZ there were 5% myelinated axons (a 95% reduction as compared to controls). After 2 weeks recovery on normal chow, 50% of the axons were myelinated, representing approximately 55% of control values. After 2 weeks recovery in the presence of LKE, 65% of the axons were myelinated, roughly 72% of control values. LKE therefore led to a 30% increase in the total percentage of myelinated axons as compared to remyelination on control chow. Treatment of control mice with LKE for 2 weeks did not affect the percentage of myelinated axons.

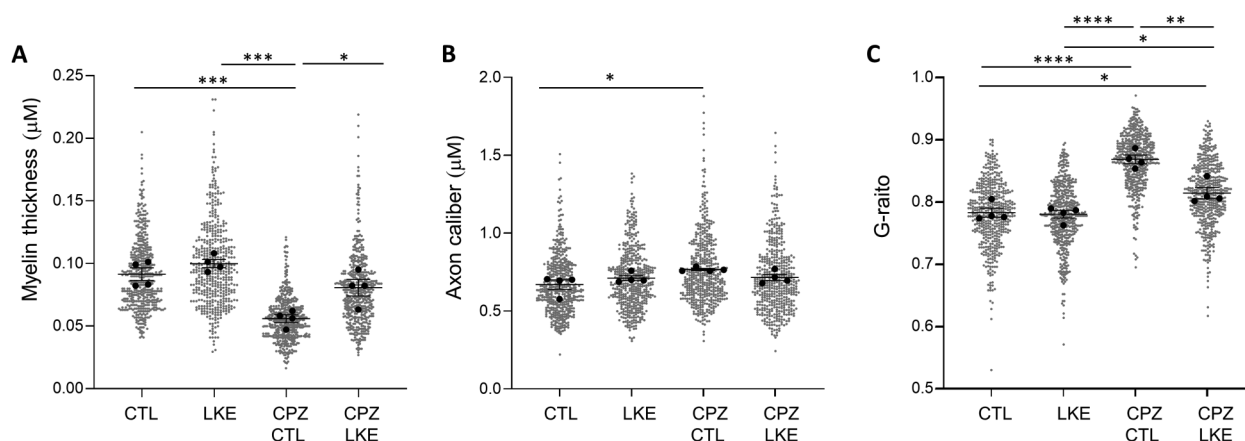


**Figure 2.** Effects of LKE on myelin thickness and axon caliber. EM images through the CC were analyzed using ImageJ to obtain values for (A) myelin thickness, (B) axon caliber, and (C) to calculate g-ratios. Data is presented for all individual axons counted (grey dots), and for average values obtained for each individual mouse (dark circles). Bars show mean  $\pm$  se. Data is derived from 4 mice per group, an average of 120 axons per mouse, and total axons of 480 (CTL), 481 (LKE), 479 (CPZ/CTL), and 482 (CPZ/LKE). 1-way ANOVA ( $F = 16.3$ ,  $P = 0.0002$  for myelin;  $F = 3.8$ ,  $P = 0.039$  for axon;  $F = 30.1$ ,  $P < 0.0001$  for g-ratio). \*,  $P < 0.05$ ; \*\*,  $P < 0.005$ ; \*\*\*,  $P < 0.0005$ ; \*\*\*\*,  $P < 0.0001$ ; Tukey multiple comparisons.

EM analysis was used to determine how remyelination in the presence of LKE affected axon caliber, myelin thickness, and g-ratios (axon caliber divided by total unit diameter). Comparison of the average values obtained for individual mice confirmed a significant reduction in myelin thickness compared to controls after 2 weeks recovery on normal chow (Figure 2A). Remyelination in the presence of LKE led to significantly thicker myelin compared to normal chow; and although slightly thinner than control values, that difference was not statistically significant. Remyelination on normal chow caused an increase in average axon caliber (Figure 2B), and that increase was absent in the LKE treated group. Comparison of g-ratios (Figure 2C) shows a significant increase following remyelination on normal chow as compared to controls, and that increase was less in the CPZ/LKE group. However, average g-ratios in the CPZ/LKE group remained slightly, but significantly higher than control g-ratios. Treatment with LKE alone had no effect on either myelin thickness, axon caliber, or g-ratio.

Examination of the frequency distribution of myelin thickness shows that remyelination on control chow led to an increase in the percentage of axons having myelin thicknesses ranging from 0.025 to 0.075 microns, and correspondingly fewer axons with myelin thickness ranging from 0.075 to 0.15 microns (Figure 3A). There were no significant differences in myelin thickness distribution between controls and the CPZ/LKE group. Compared to the CPZ/CTL group, the CPZ/LKE group had fewer axons with thin myelin (0.025 to 0.075 microns) and more axons with myelin from 0.075 to 0.10 microns. The increase in average axon caliber (Figure 2B) following normal remyelination can be attributed to a decrease in the percentage of smaller axons (ranging from 0.25 to 0.50 microns) (Figure 3B). The distribution of g-ratios (Figure 3C) was strongly right shifted after normal

remyelination, with significant reductions in axons having smaller g-ratios and significant increases in axons with larger g-ratios. Remyelination in the presence of LKE tended to restore g-ratios to the control distribution, however, there remained fewer axons with g-ratios in the 0.69–0.77 range, and more axons with g-ratios in the 0.85 to 0.89 range. G-ratios in the CPZ/LKE group were strongly left shifted compared to the CPZ/CTL group.

Scatter plots of g-ratio versus axon caliber (Figure 4A) show that the larger g-ratios following normal remyelination occurred across all axon sizes, and that the effect of LKE during recovery on reducing g-ratios also occurred at all axon sizes. LKE treatment of control mice had only a minor effect on g-ratios. To better determine if LKE influenced all axons, we calculated the average myelin thickness in different axon caliber ranges (Figure 4B). In controls, the average myelin thickness showed a close to linear association with increasing axon caliber. After 2 weeks remyelination on normal chow, the average myelin thickness was restored to approximately the same extent (0.05  $\mu$ m) across all axons, which may reflect a similar modest degree of remyelination occurring on all axons. However, following 2 weeks remyelination in the presence of LKE, the association of myelin thickness to axon size was restored. This suggests that accelerated remyelination due to LKE replicates controls, such that smaller axons are not hypermyelinated nor larger axons hypomyelinated. This is further illustrated (Figure 4C) by restoration of g-ratios by LKE towards control values across all axon size ranges.

Immunohistochemical staining was carried out to determine if LKE affected myelin protein expression (Figure 5). For these studies we included samples from mice treated with CPZ for 5 weeks, a group not included in EM analyses since essentially all axons are demyelinated at that time.



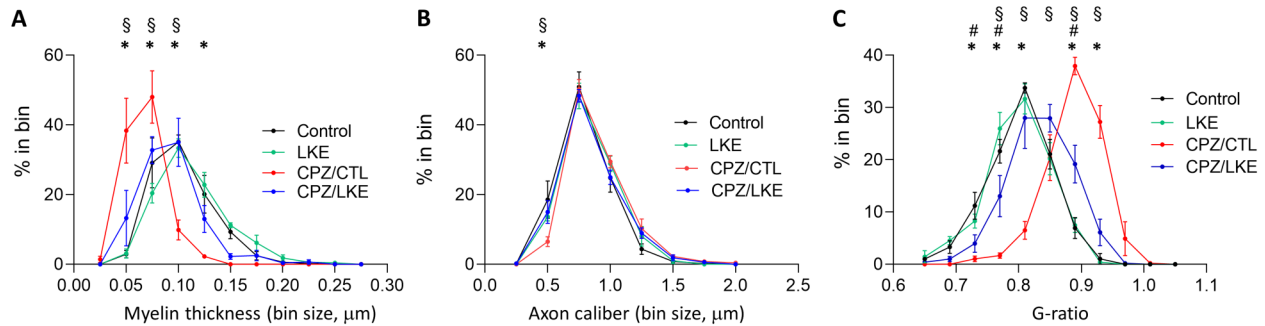


**Figure 3.** LKE restores distribution of myelin thickness and g-ratios during remyelination. Histograms of the frequency distributions of (A) myelin thickness, (B) axon caliber and (C) g-ratios were generated for each individual mouse. Data is mean  $\pm$  SE of the percentage of axons in each bin,  $n = 4$  mice per group. For myelin thickness, bin size is 0.025 microns, e.g. axons in bin 0.05 range from 0.025 to 0.050 microns. For axon caliber the bin size is 0.25 microns, e.g. axons in bin 0.50 range from 0.25 to 0.50 microns. For g-ratios the bin size is 0.04, e.g. axons in bin 0.69 have g-ratios from 0.65 to 0.69. 2-way ANOVA, 2-way interactions were  $F(30,132) = 7.1$ ,  $P < 0.0001$  for myelin thickness;  $F(30,132) = 16.3$ ,  $P < 0.001$  for g-ratio; and  $F(21,96) = 1.3$ ,  $P = 0.167$  for axon caliber. \*,  $P < 0.05$  CTL versus CPZ/CTL; #,  $P < 0.05$  CTL versus CPZ/LKE; §,  $P < 0.05$  CPZ/CTL versus CPZ/LKE, Tukey multiple comparisons.

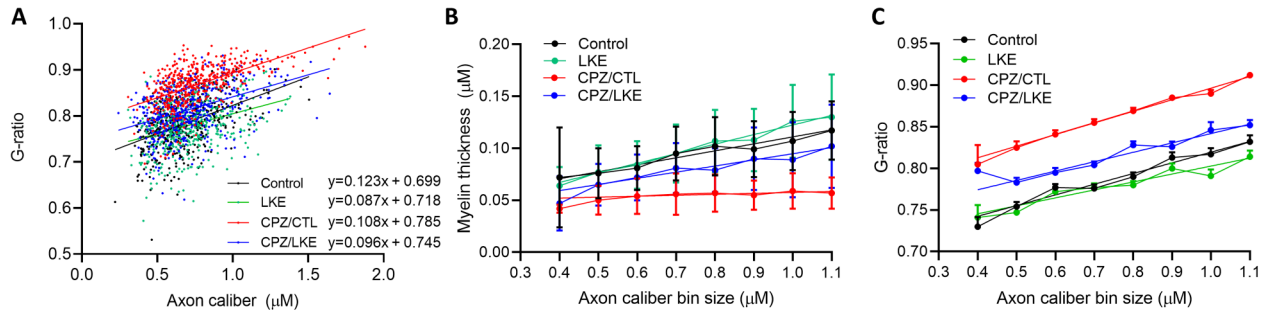


**Figure 4.** LKE increases myelin thickness and g-ratios across all axon sizes. (A) Scatter graphs of g-ratio versus axon caliber for all axons in all groups. The data was fit by simple linear regression, slopes and intercepts are indicated. (B) Average myelin thickness and (C) average g-ratios for axons in the indicated bins were determined for each mouse. Axon bin size is 0.1 microns, axons in the 0.4 bin have calibers from 0.3 to 0.4 microns. Data is mean  $\pm$  SE of  $n = 4$  mice per group.

Measurements were made both in the CC as well as the overlying somatosensory cortical (CX) region. Staining for myelin proteins MBP and PLP shows that CPZ significantly reduced their staining in both brain regions (Figure 5C–F). After 2 weeks remyelination on normal chow, there was a modest increase of MBP in the CC (Figure 5D), and of PLP in both CX and CC (Figure 5E and F) as compared to CPZ. However those increases were not significantly different from values measured in the CPZ group. In contrast, after 2 weeks of remyelination in the presence of LKE there were significant increases in both MBP and PLP in both CC and CX, as compared to the CPZ group. While staining intensities for MBP and PLP were always greater in the CPZ/LKE groups than the CPZ/CTL groups, those differences did not reach statistical significance except for PLP staining in the CC. In contrast to modest increases observed in MBP and PLP staining intensity on CTL chow, the relative mRNA levels of MBP and PLP were both significantly increased after 2 weeks recovery as compared to the highly reduced levels in the CPZ group (Figure 6A and B).

We carried out immunohistochemical staining to determine if LKE affected OLG maturation or proliferation (Figure 7A). Staining for Olig2 and CC1 was quantified only in the CX since the density of Olig2<sup>+</sup> and CC1<sup>+</sup> cells in the CC is too high to get accurate values. Olig2 staining showed that CPZ significantly reduced the total number of OLGs in the CX, that those numbers were slightly increased after 2 weeks recovery on normal chow, but were restored to normal levels after 2 weeks remyelination in the presence of LKE (Figure 7B). Despite significant changes seen in Olig2<sup>+</sup> cell numbers, relative Olig2 mRNA levels were only modestly reduced after 5 weeks of CPZ treatment, however those levels were significantly increased following recovery on LKE chow (Figure 6C). The number of CC1<sup>+</sup> post-mitotic (pre-myelinating and myelinating) cells was reduced by CPZ, not significantly increased after 2 weeks on normal chow, and fully restored by recovery on LKE chow (Figure 7D). The percentage of [Olig2<sup>+</sup> : CC1<sup>+</sup>] double-labeled cells (post mitotic OLGs) was greatly reduced by CPZ, was not significantly increased after 2 weeks of remyelination on

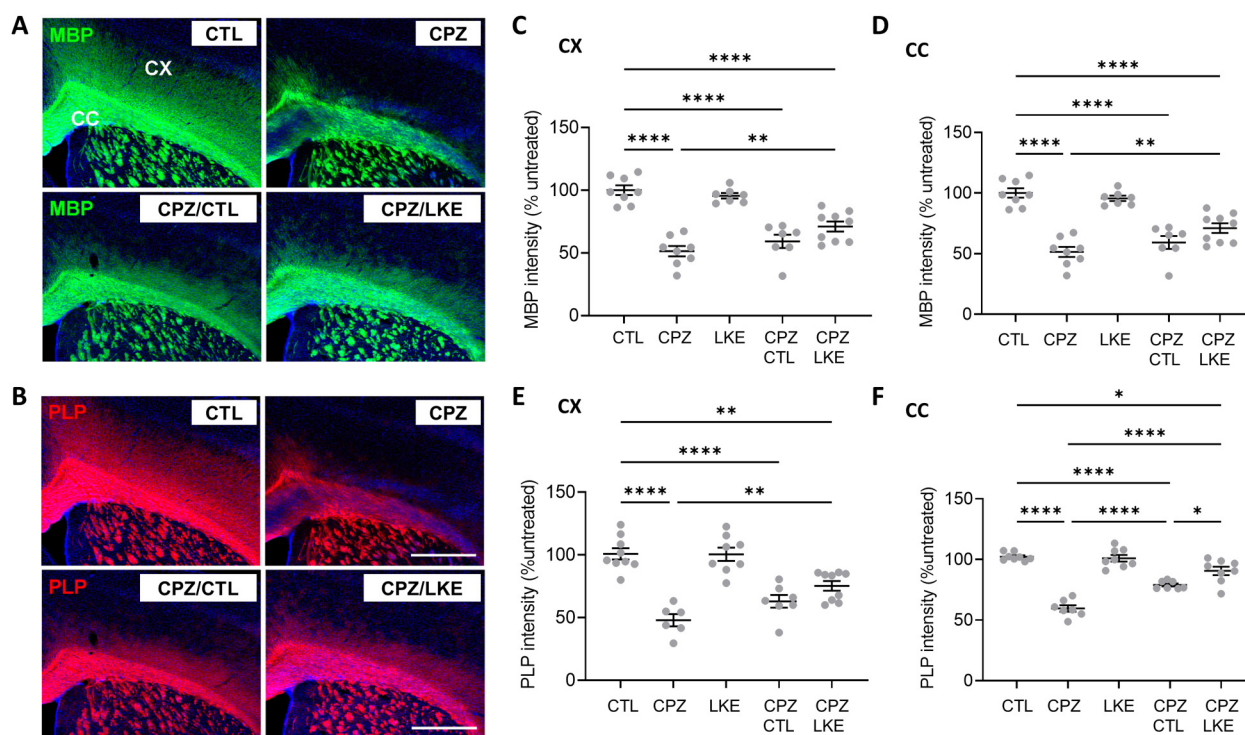


**Figure 5.** LKE increases myelin protein expression during remyelination. Representative sections through the CC and overlying somatosensory cortex (CX) stained for (A) MBP and (B) PLP from CTL, CPZ, LKE, CPZ/CTL, and CPZ/LKE mice. (C, D) MBP and (E, F) PLP staining was quantified in the CX and CC. Data is % staining intensity relative to staining in CTL samples, and is mean  $\pm$  SE  $n = 7-9$  mice per group except for PLP in the CX for the CPZ group ( $n = 6$ ). 1-way ANOVA  $F = 28.9$  for MBP in CX;  $F = 20.6$  for MBP in CC;  $F = 22.1$  for PLP in CX; and  $F = 50.1$  for PLP in CC. Significance was  $P < 0.0001$  for C-F \*,  $P < 0.05$ ; \*\*,  $P < 0.005$ ; \*\*\*,  $P < 0.0005$ , \*\*\*\*,  $P < 0.0001$ ; Tukey's multiple comparison tests. Scale bar represents 200 microns.

control chow, but was significantly increased after recovery on LKE chow (Figure 7C). Co-staining for double-labeled [Olig2<sup>+</sup> : Ki67<sup>+</sup>] cells (Figure 7D) shows that CPZ increased the percentage of proliferating cells, but that was not significantly altered following 2 weeks remyelination on control or LKE containing chow. Taken together these results suggest that the effects of LKE on OPC and OLG cell numbers was not due to increased proliferation but instead to increased survival and/or maturation.

To determine if the actions of LKE involved effects on glial cell activation or number, we stained sections for expression of GFAP and Iba1 (Figure 8A and B). As for Olig2 and CC1, quantitation of GFAP+ and Iba1+ cell numbers was done only for CX since their density in the CC was too high to get accurate values. GFAP staining was significantly increased by CPZ in both the CX and CC (Figure 8C and D) as were the number of GFAP+ stained cells in the CX (Figure 9C). Compared to the CPZ group, both GFAP staining and the number of GFAP+ stained cells in the CX decreased following recovery on either control or LKE chow, to similar extents. In contrast, GFAP staining was not reduced in the CC after recovery. Quantitation of relative GFAP mRNA levels confirmed an increase in GFAP mRNA due to CPZ, but no significant reductions following

recovery (Figure 6D). Staining for the microglial marker Iba1 showed no increase in staining intensity due to CPZ in the CX. Although Iba1 staining was increased by CPZ in the CC (Figure 8F), that did not reach statistical significance compared to the CTL group. The number of Iba1+ cells was increased in the CX by CPZ (Figure 9D), and although not statistically significant by 1-way ANOVA, it was significant by T-test or when either the highest or lowest value for CPZ/LKE was omitted. Nevertheless, neither Iba1 staining intensity nor cell numbers changed after 2 weeks recovery. In contrast, we observed a significant increase in relative Iba1 mRNA levels due to CPZ, and that was restored to close to CTL levels after 2 weeks recovery (Figure 6E).

## Discussion

In the current study we provided mice a diet containing 0.2% CPZ, and found after 5 weeks there was demyelination of 95% of axons in the caudal CC. This is consistent with findings from several other groups of almost complete demyelination in this area of the CC between 4 to 5 weeks of CPZ treatment (Mason et al., 2001; Matsushima & Morell, 2001; Steelman et al., 2012; Taylor et al., 2010; Xie et al., 2010). This degree of demyelination is greater than observed after

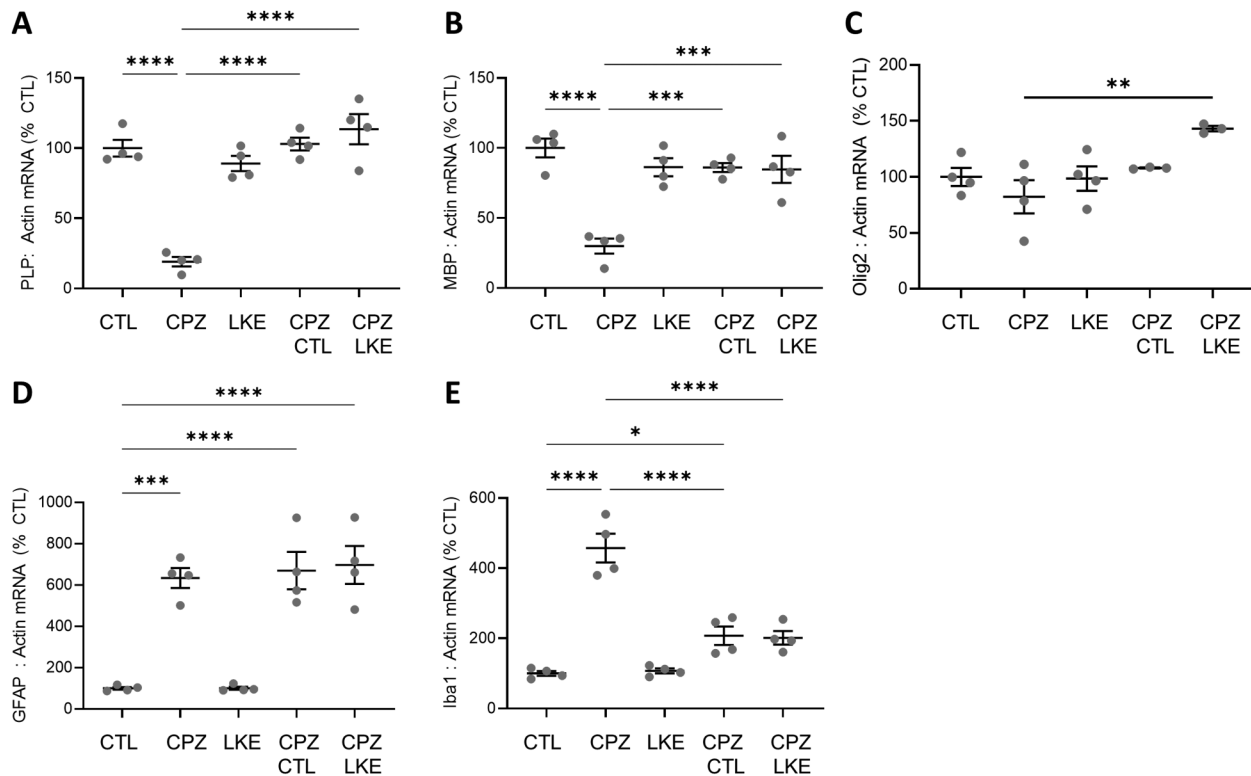


**Figure 6.** Effects of LKE on oligodendrocyte and glial mRNA levels. Relative mRNA levels in the CC were determined by qPCR in samples from CTL, CPZ, LKE, CPZ/CTL, and CPZ/LKE mice for (A) GFAP; (B) PLP; (C) MBP; (D) GFAP; and (E) Iba1. Data is mean  $\pm$  SE of  $n = 4$  mice per group and is mRNA levels normalized to  $\beta$ -actin measured in the same samples, shown relative to CTL values (100%). 1-way ANOVA  $F = 3.3$  for Olig2;  $F = 36.4$  for PLP;  $F = 17.0$  for MBP;  $F = 25.4$  for GFAP; and  $F = 36.8$  for Iba1. \*,  $P < 0.05$ ; \*\*\*\*,  $P < 0.0001$  versus CTL. Tukey's multiple comparison tests.

longer treatment periods with CPZ due to remyelination beginning as early as week 5 even in the presence of CPZ (Lindner et al., 2008).

### Effects of LKE on Remyelination

Following 2 weeks recovery in the absence of CPZ, the percent of myelinated axons increased to 50%, representing approximately 55% of control values. In contrast, recovery in the presence of LKE was greater, and increased the percentage of myelinated fibers to 65%, which represents 72% of control values. Thus, while LKE significantly increased remyelination, after 2 weeks a large number of naked axons remained. However, results from several other laboratories suggest that remyelination up to 70% of control values may be the maximum achievable. For example, in the body of the CC, recovery for 2 weeks led to 60% myelinated fibers, and increased to about 70% after 4 weeks (Santiago Gonzalez et al., 2017). In the splenium of the CC, 2 weeks recovery increased the percentage of myelinated fibers from almost 0% to about 50% (Steelman et al., 2012). Lower extents of remyelination have also been reported, for example in the dorsal CC where after 2 weeks recovery only 20% of control values were reached (Steelman et al.,

2012); with only 40% of the fibers myelinated across the whole CC (Wasko et al., 2019). While some variability exists in the degree of remyelination occurring after short times of recovery and in different regions and sub-regions, long term recovery appears to be limited to about 70% myelinated axons even after 12 weeks (Gingele et al., 2020; Hibbits et al., 2009; Mason et al., 2001). Therefore 2 weeks recovery in the presence of LKE may already be at or near maximal levels of remyelination.

### Effects of LKE on OLG Numbers and Maturation

As expected, 5 weeks of CPZ treatment significantly reduced the total number of OLGs (Olig2<sup>+</sup> cells) and the density of mature myelinating cells (CC1<sup>+</sup> cells) in the cortex. These changes were associated with a rise in the percentage of proliferating double labeled [Olig2<sup>+</sup> : Ki67<sup>+</sup>] OPCs and with a reduction in the percentage of mature double labeled [Olig2<sup>+</sup> : CC1<sup>+</sup>] OLGs in the entire population. Two weeks of normal diet partially restored Olig2<sup>+</sup> and CC1<sup>+</sup> cell numbers in control animals, however, LKE treated mice showed a nearly complete recovery of both Olig2<sup>+</sup> and CC1<sup>+</sup> cell densities in the cortex. The faster recovery of the OLG population is likely responsible for the more



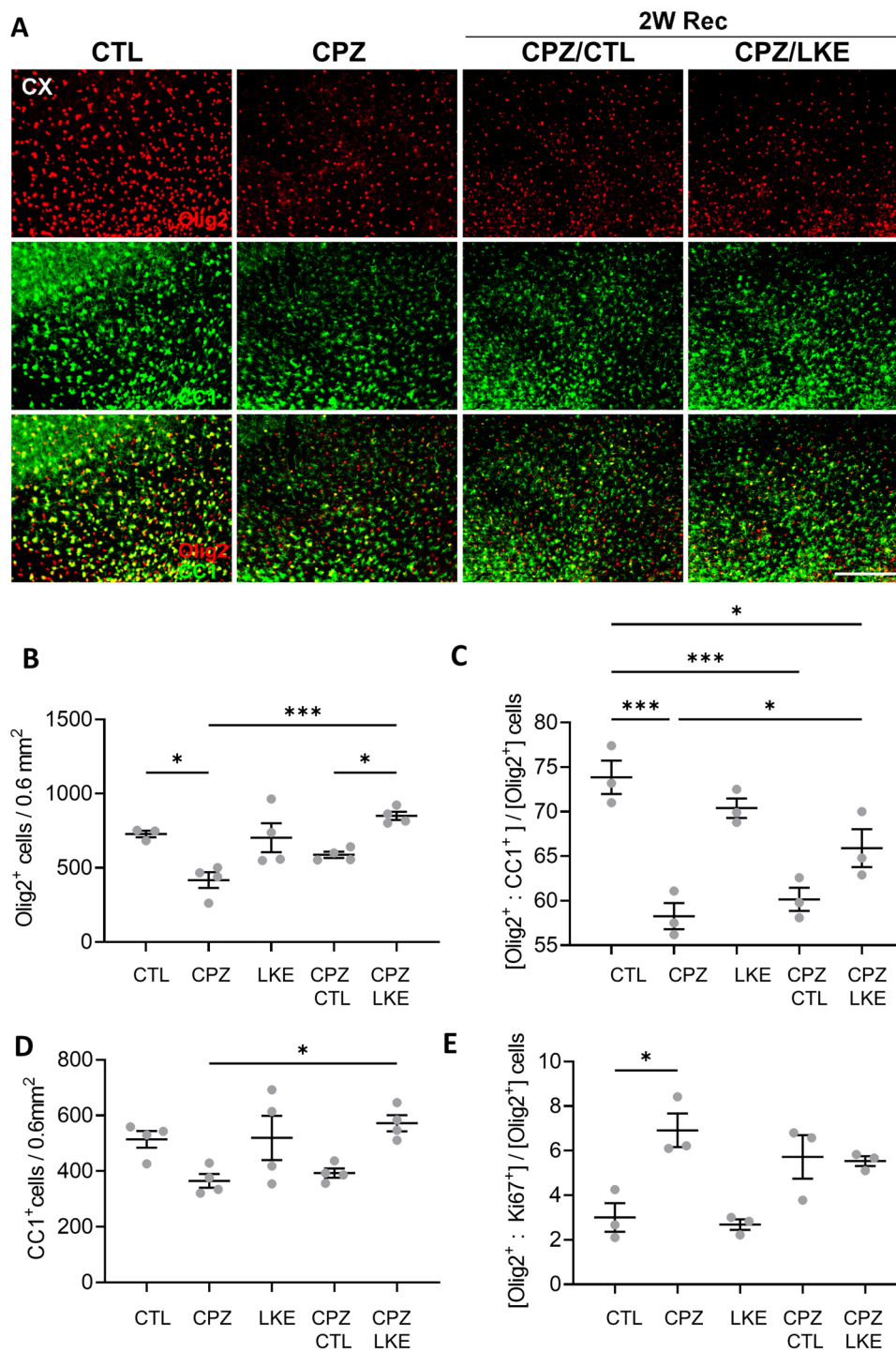


**Figure 7.** LKE increases OLG cell numbers and OPC maturation during remyelination. (A) Representative sections through the CC and overlying somatosensory cortex (CX) stained for Olig2 and CCI from CTL, CPZ, CPZ/CTL, and CPZ/LKE mice. Quantitation of (B) Number of Olig2<sup>+</sup> cells; (C) Percentage of double-labeled [Olig2<sup>+</sup> : Ki67<sup>+</sup>] cells out of total Olig2<sup>+</sup> cells; (D) Number of CCI<sup>+</sup>; and (E) Percentage of double labeled [Olig2<sup>+</sup> : CCI<sup>+</sup>] cells, out of total Olig2<sup>+</sup> cells. Data is mean  $\pm$  SE of n = 3 or 4 mice per group. 1-way ANOVA F = 6.6 for Olig2<sup>+</sup>; F = 4.9 for CCI<sup>+</sup>; F = 8.3 for Olig2:Ki67; and F = 16.7 for Olig2<sup>+</sup>:CCI<sup>+</sup>. Significance was P < 0.0001 for B–E. \*, P < 0.05; \*\*\*, P < 0.0001 versus CTL. Tukey's multiple comparison tests. Scale bar represents 200 microns.

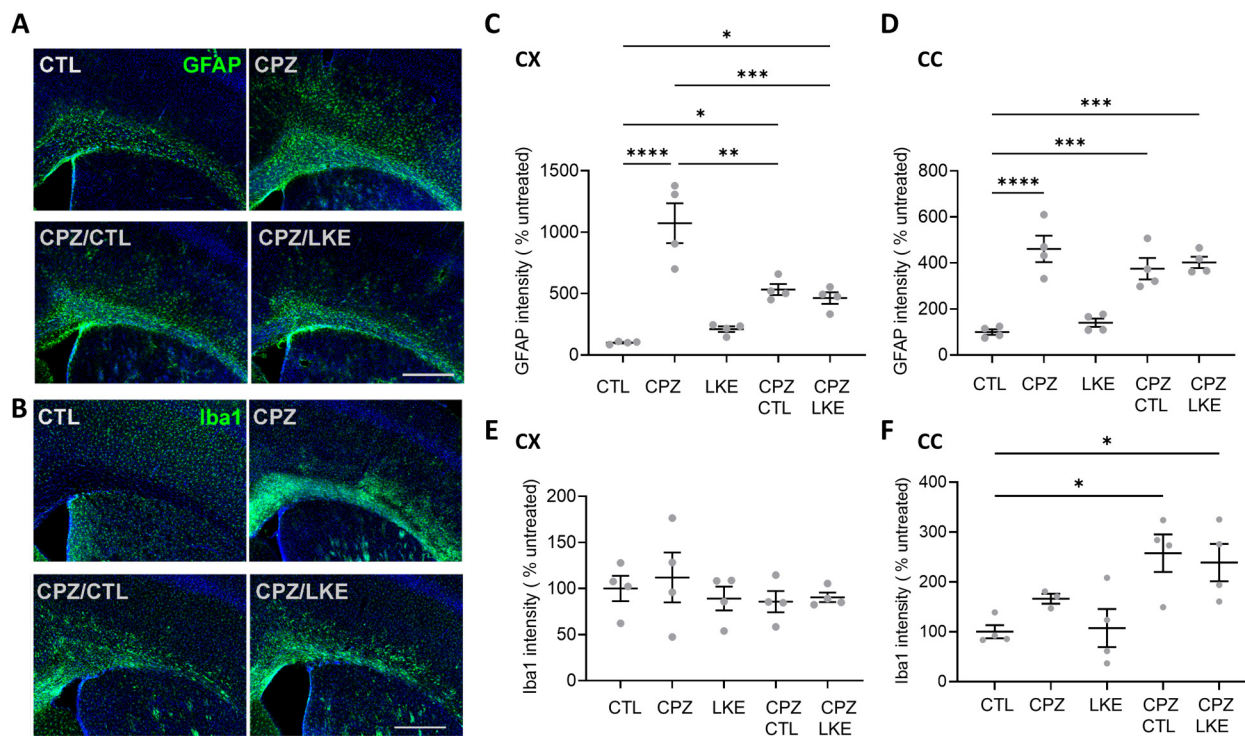


**Figure 8.** LKE does not reduce glial cell activation during remyelination. Representative sections through the CC and overlying somatosensory cortex (CX) stained for (A) GFAP and (B) Iba1 from CTL, CPZ, LKE, CPZ/CTL, and CPZ/LKE mice. (C, D) GFAP and (E, F) Iba1 staining was quantified in the CX and CC. Data is % staining intensity relative to CTL samples, and is mean  $\pm$  SE  $n=4$  mice per group. 1-way ANOVA  $F=23.0$  for GFAP in CX;  $F=20.5$  for GFAP in CC;  $F=0.5$  for Iba1 in CX;  $F=5.5$  for Iba1 in CC. Significance was  $P < 0.0001$  for B, C, D; and  $P < 0.05$  for E, G. \*,  $P < 0.05$ ; \*\*,  $P < 0.005$ ; \*\*\*,  $P < 0.0005$ ; \*\*\*\*,  $P < 0.0001$ ; Tukey's multiple comparison tests. Scale bar represents 200 microns.

efficient remyelination observed in the LKE treatment group. Since no changes in proliferation of [Olig2<sup>+</sup> : Ki67<sup>+</sup>] OPCs were detected comparing recovery on control versus LKE chow, the increased numbers of Olig2<sup>+</sup> and CC1<sup>+</sup> positive cells in LKE treated animals are most likely a consequence of an enhanced OPC/OLG survival and maturation.

### Limited Effects of LKE on Glial Cell Activation

Several studies have also demonstrated that LKE can suppress glial activation suggesting this may contribute to LKE ability to enhance remyelination. LKE reduced microglial activation in vitro (Hensley et al., 2010a) as well as in vivo in mouse models of PD (Togashi et al., 2020); spinal cord injury (Kotaka et al., 2017); and AD (Hensley et al., 2013). Both astrocyte and microglial responses have been shown to modulate remyelination in the CPZ model (Gudi et al., 2014; Sen et al., 2022). Phagocytosis of myelin debris (Cignarella et al., 2020; Ding et al., 2021; Shen et al., 2021) and production of protective factors (Aryanpour et al., 2021) can enhance remyelination, while production of inflammatory mediators can impede remyelination (Thomas & Pasquini, 2018). Microglial ablation using antagonists of the CSF1R show

increased remyelination (Tahmasebi et al., 2021); as did astrocyte ablation using La-amino adipate (Madadi et al., 2019). Reducing Ca<sup>2+</sup> influx into astrocytes has been shown to reduce both astrocyte and microglial activation, as well as promote remyelination (Zamora et al., 2020); suggesting that actions of LKE on voltage gated Ca<sup>2+</sup> channels could contribute to its actions. However, while we observed increases in both astrocyte (GFAP) and microglial (Iba1) expression following CPZ treatment, after 2 weeks of recovery those increases were diminished to a similar extent on LKE and CTL chow. It remains possible that LKE influenced glial cell responses at an earlier time point; or that measurements of other markers of glial activation involved in inflammatory or phagocytosis responses, would reveal LKE dependent actions.

### Mechanisms of Action and Targets of LKE

The mechanisms by which LKE increases remyelination remain to be determined. Proteomic studies (Hensley et al., 2010a) identified a primary binding target of LKE as CRMP2 (Collapsin Response Mediator Protein 2). CRMP2 is well characterized with respect to stimulation of neuriteogenesis and axonal guidance involving binding to  $\alpha$ -tubulin and

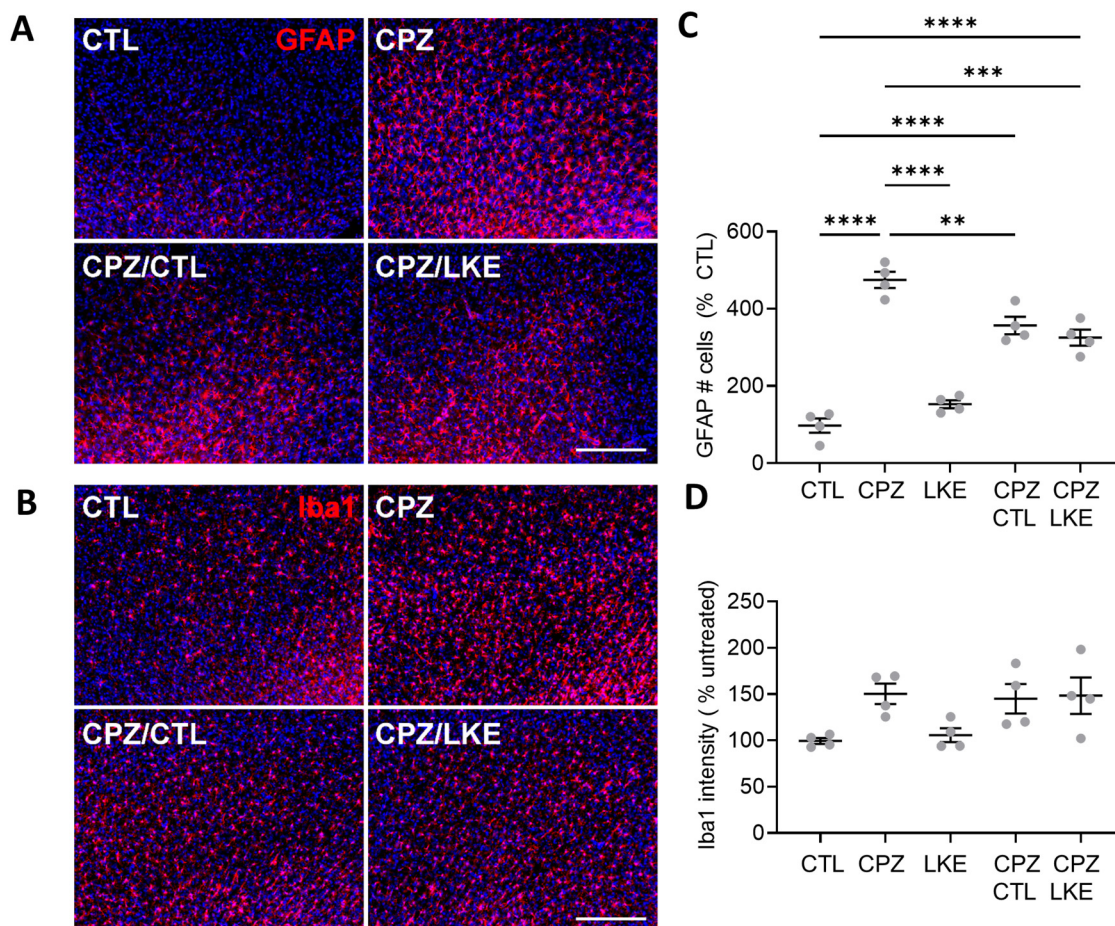


**Figure 9.** LKE does not reduce glial cell numbers during remyelination. Representative sections through the somatosensory cortex stained for (A) GFAP and (B) Iba1 from CTL, CPZ, LKE, CPZ/CTL, and CPZ/LKE mice. Data is % cell numbers (C, D) relative to CTL samples, and is mean  $\pm$  SE  $n = 4$  mice per group. 1-way ANOVA  $F = 64.9$  for GFAP;  $F = 3.8$  for Iba1. Significance was  $P < 0.05$  for C. \*,  $P < 0.05$ ; \*\*,  $P < 0.005$ ; \*\*\*,  $P < 0.0005$ , \*\*\*\*,  $P < 0.0001$ ; Tukey's multiple comparison tests. Scale bar represents 90 microns.

growth of microtubules (Kotaka et al., 2017). CRMP2 binding is regulated by phosphorylation, including at Serine 522 by cyclin dependent kinase 5 (Cdk5) (Uchida et al., 2005) which reduces CRMP2's affinity for tubulin and so reduces microtubule growth. LKE increases CRMP2 function (Hensley et al., 2010a, 2010b) by reducing Cdk5-mediated phosphorylation (Fernandez-Gamba et al., 2012; Wilson et al., 2014). While primarily expressed in neurons in the adult brain, CRMP2 is also expressed in OLGs, and roles in OLG survival, maturation and process extension have been reported (Piaton et al., 2011; Syed et al., 2017). Moreover, in mice with a non-phosphorylatable CRMP2, myelin protein expression is increased (Nakamura et al., 2018), consistent with the possibility that some actions of LKE on remyelination are due to reducing CRMP2 phosphorylation. Findings that CRMP2 has roles in mediating optic nerve damage (Mimura et al., 2006; Petratos et al., 2012); and reduces clinical signs and neuroinflammation (Moutal et al., 2019) in EAE further supports a role for CRMP2 in mediating LKE actions.

In addition to tubulin, CRMP2 also interacts with the N-type voltage gated calcium channel Cav2.2, targeting it to neuronal membranes (Brittain et al., 2009). CRMP2 phosphorylation by Cdk5 increases that association, thereby increasing  $Ca^{2+}$  influx and neurotransmitter release (Chi et al., 2009). Roles for Cav2.2 in MS are suggested by findings that in lesions, the  $\alpha 1B$  subunit of Cav2.2 accumulates in damaged axons (Kornek et al., 2001). The  $\alpha 1B$  subunit also accumulates in demyelinated axons in a rat model of optic neuritis, and treatment with the Cav2.2 inhibitor omega-conotoxin reduced axon and myelin damage (Gadjanski et al., 2009). Similarly,  $\alpha 1B$  null mice show reduced clinical signs of EAE and demyelination than wild type mice (Tokuhara et al., 2010); and treatment of EAE with a Cav2.2 blocker (Silva et al., 2018) ameliorated clinical signs and neuroinflammation. CRMP2 also interacts with GluN2B containing N-methyl-D-aspartate NMDA receptors (NMDARs) (Bretin et al., 2006; Moutal et al., 2014), and disruption of those interactions reduces NMDAR-mediated  $Ca^{2+}$  currents and affords neuroprotection in ischemia and traumatic brain injury models (Brittain et al.,



2012; Brustovetsky et al., 2014). NMDARs are also expressed on OLG processes and in myelin (Matute, 2011), and broad-spectrum NMDAR antagonists (AP5, MK801) blocked  $\text{Ca}^{2+}$  accumulation into myelin and reduced myelin damage in the optic nerve (Matute, 2010). Several studies have also reported that NMDAR antagonists are protective in EAE (Dąbrowska-Bouta et al., 2015; Farjam et al., 2014; Wallström et al., 1996). Together these findings suggest that by reducing CRMP2 phosphorylation, LKE could decrease CRMP2 interactions with Cav2.2 or NMDARs, thereby reducing  $\text{Ca}^{2+}$  influx under conditions when excessive  $\text{Ca}^{2+}$  influx leads to cell death or damage (Brittain et al., 2012).

In summary, the current study demonstrates that LKE, a semi-synthetic derivative of the naturally occurring, non-proteogenic amino acid lanthionine, accelerates the remyelination process in the CPZ mouse model of MS. However, several questions remain unanswered. The CPZ model shows minimal involvement of the peripheral adaptive immune responses, however roles for both astrocyte (Gudi et al., 2014) and microglial (Vega-Riquer et al., 2019) activation have been reported. Since LKE has previously been shown to reduce microglial activation (Hensley et al., 2010a, 2013; Kotaka et al., 2017; Togashi et al., 2020), it remains to be determined if LKE effects on remyelination also involve suppression of glial cell responses. It also is important to determine if remyelination in the presence of LKE leads to restoration of correct nodal, paranodal, and internodal structure; and most critically if functional recovery is achieved, for example by restoration of compound action potentials across the CC. Finally, as mentioned above, the precise mechanisms of action of LKE which lead to increased OLG survival or OPC maturation, including the relative importance of CRMP2, Cav2.2, and NMDARs, should be elucidated.

### Declaration of Conflicting Interests


The author(s) declared no potential conflicts of interest with respect to the research, authorship, and/or publication of this article.

### Funding

The author(s) disclosed receipt of the following financial support for the research, authorship, and/or publication of this article: This work was supported by the National Institutes of Health (grant numbers R01-NS081141-01A1 and 5R01-NS111552-02) to STW, the U.S. Department of Veterans Affairs (grant numbers 14S-RCS-003 to DLF, and 1101BX002565-06 to JLD), the Washington Research Foundation (Technology Commercialization grant to TD), and the National Multiple Sclerosis Society (grant numbers RG-1501-02654 to DLF, RG-1807-31649 to PP, and RG-1901-33349 to STW).

### ORCID iDs

Pablo M. Paez  <https://orcid.org/0000-0001-9362-9454>

Seema K. Tiwari-Woodruff  <https://orcid.org/0000-0001-7608-4763>

Douglas L. Feinstein  <https://orcid.org/0000-0003-2815-2885>

### Supplemental Material

Supplemental material for this article is available online.

### References

- Aryanpour, R., Zibara, K., Pasbakhsh, P., Namjoo, S. B., Ghanbari, Z., Mahmoudi, A., Amani, R., & Kashani, S. (2021). 17 $\beta$ -Estradiol reduces demyelination in cuprizone-fed mice by promoting M2 microglia polarity and regulating NLRP3 inflammatory. *Neuroscience*, *463*, 116–127. <https://doi.org/10.1016/j.neuroscience.2021.03.025>.
- Bretin, S., Rogemond, V., Marin, P., Maus, M., Torrens, Y., Honnorat, J., Glowinski, J., Premont, J., & Gauchy, C. (2006). Calpain product of wt-crm2 reduces the amount of surface nr2b nmda receptor subunit. *Journal of Neurochemistry*, *98*(4), 1252–1265. <https://doi.org/10.1111/j.1471-4159.2006.03969.x>
- Brittain, J. M., Pan, R., You, H., Brustovetsky, T., Brustovetsky, N., Zamponi, G. W., Lee, W. H., & Khanna, R. (2012). Disruption of nmdar-crm2 signaling protects against focal cerebral ischemic damage in the rat middle cerebral artery occlusion model. *Channels (Austin)*, *6*(1), 52–59. <https://doi.org/10.4161/chan.18919>
- Brittain, J. M., Piekarz, A. D., Wang, Y., Kondo, T., Cummins, T. R., & Khanna, R. (2009). An atypical role for collapsin response mediator protein 2 (crm2) in neurotransmitter release via interaction with presynaptic voltage-gated calcium channels. *Journal of Biological Chemistry*, *284*(45), 31375–31390. <https://doi.org/10.1074/jbc.M109.009951>
- Brustovetsky, T., Pellman, J. J., Yang, X. F., Khanna, R., & Brustovetsky, N. (2014). Collapsin response mediator protein 2 (crm2) interacts with n-methyl-d-aspartate (nmda) receptor and na<sup>+</sup>/ca<sup>2+</sup> exchanger and regulates their functional activity. *Journal of Biological Chemistry*, *289*(11), 7470–7482. <https://doi.org/10.1074/jbc.M113.518472>
- Chang, A., Tourtellotte, W. W., Rudick, R., & Trapp, B. D. (2002). Premyelinating oligodendrocytes in chronic lesions of multiple sclerosis. *New England Journal of Medicine*, *346*(3), 165–173. <https://doi.org/10.1056/NEJMoa010994>
- Chi, X. X., Schmutzler, B. S., Brittain, J. M., Wang, Y., Hingtgen, C. M., Nicol, G. D., & Khanna, R. (2009). Regulation of n-type voltage-gated calcium channels (cav2.2) and transmitter release by collapsin response mediator protein-2 (crm2) in sensory neurons. *Journal of Cell Science*, *122*(Pt 23), 4351–4362. <https://doi.org/10.1242/jcs.053280>
- Cignarella, F., Filipello, F., Bollman, B., Cantoni, C., Locca, A., Mikesell, R., Manis, M., Ibrahim, A., Deng, L., Benitez, B. A., Cruchaga, C., Licastro, D., Mihindikulasuriya, K., Harari, O., Buckland, M., Holtzman, D. M., Rosenthal, A., Schwabe, T., Tassi, I., & Piccio, L. (2020). TREM2 activation on microglia promotes myelin debris clearance and remyelination in a model of multiple sclerosis. *Acta Neuropathologica*, *140*(4), 513–534. <https://doi.org/10.1007/s00401-020-02193-z>
- Clark, K. C., Josephson, A., Benusa, S. D., Hartley, R. K., Baer, M., Thummala, S., Joslyn, M., Sword, B. A., Elford, H., Oh, U., Dilsizoglu-Senol, A., Lubetzki, C., Davenne, M., DeVries, G. H., & Dupree, J. L. (2016). Compromised axon initial segment integrity in eae is preceded by microglial reactivity and contact. *Glia*, *64*(7), 1190–1209. <https://doi.org/10.1002/glia.22991>
- Dąbrowska-Bouta, B., Strużyńska, L., Chalimoniuk, M., Frontczak-Baniewicz, M., & Sulkowski, G. (2015). The influence of glutamatergic receptor antagonists on biochemical and

- ultrastructural changes in myelin membranes of rats subjected to experimental autoimmune encephalomyelitis. *Folia Neuropathologica*, 53(4), 317–326. <https://doi.org/10.5114/fn.2015.56546>
- Ding, Z. B., Han, Q. X., Wang, Q., Song, L. J., Chu, G. G., Guo, M. F., Chai, Z., Yu, J. Z., Xiao, B. G., Li, X. Y., & Ma, C. G. (2021). Fasudil enhances the phagocytosis of myelin debris and the expression of neurotrophic factors in cuprizone-induced demyelinating mice. *Neuroscience Letters*, 753, 135880.
- Dupree, J. L., & Feinstein, D. L. (2018). Influence of diet on axonal damage in the eae mouse model of multiple sclerosis. *Journal of Neuroimmunology*, 322, 9–14. <https://doi.org/10.1016/j.jneuroim.2018.05.010>
- Dupree, J. L., Polak, P. E., Hensley, K., Pelligrino, D., & Feinstein, D. L. (2015). Lanthionine ketimine ester provides benefit in a mouse model of multiple sclerosis. *Journal of Neurochemistry*, 134(2), 302–314. <https://doi.org/10.1111/jnc.13114>
- Farjam, M., Beigi Zarandi, F. B., Farjadian, S., Geramizadeh, B., Nikseresht, A. R., & Panjehshahin, M. R. (2014). Inhibition of nr2b-containing n-methyl-d-aspartate receptors (nmdars) in experimental autoimmune encephalomyelitis, a model of multiple sclerosis. *Iranian Journal of Pharmaceutical Research*, 13(2), 695–705.
- Fernandez-Gamba, A., Leal, M. C., Maarouf, C. L., Richter-Landsberg, C., Wu, T., Morelli, L., Roher, A. E., & Castano, E. M. (2012). Collapsin response mediator protein-2 phosphorylation promotes the reversible retraction of oligodendrocyte processes in response to non-lethal oxidative stress. *Journal of Neurochemistry*, 121(6), 985–995. <https://doi.org/10.1111/j.1471-4159.2012.07742.x>
- Franklin, K., & Paxinos, G. (2008). The mouse brain in stereotaxic coordinates. 256.
- Gadjanski, I., Boretius, S., Williams, S. K., Lingor, P., Knoferle, J., Sattler, M. B., Fairless, R., Hochmeister, S., Suhs, K. W., Michaelis, T., Frahm, J., Storch, M. K., Bahr, M., & Diem, R. (2009). Role of n-type voltage-dependent calcium channels in autoimmune optic neuritis. *Annals of Neurology*, 66(1), 81–93. <https://doi.org/10.1002/ana.21668>
- Gingele, S., Henkel, F., Heckers, S., Moellenkamp, T. M., Hümmert, M. W., Skripuletz, T., Stangel, M., & Gudi, V. (2020). Delayed demyelination and impaired remyelination in aged mice in the cuprizone model. *Cells*, 9(4), 945. <https://doi.org/10.3390/cells9040945>
- Gudi, V., Gingele, S., Skripuletz, T., & Stangel, M. (2014). Glial response during cuprizone-induced de- and remyelination in the CNS: lessons learned. *Frontiers in Cellular Neuroscience*, 8, 73. <https://doi.org/10.3389/fncel.2014.00073>
- Hensley, K., Christov, A., Kamat, S., Zhang, X. C., Jackson, K. W., Snow, S., & Post, J. (2010a). Proteomic identification of binding partners for the brain metabolite lanthionine ketimine (lk) and documentation of lk effects on microglia and motoneuron cell cultures. *Journal of Neuroscience*, 30(8), 2979–2988. <https://doi.org/10.1523/JNEUROSCI.5247-09.2010>
- Hensley, K., & Denton, T. T. (2015). Alternative functions of the brain transsulfuration pathway represent an underappreciated aspect of brain redox biochemistry with significant potential for therapeutic engagement. *Free Radical Biology and Medicine*, 78, 123–134. <https://doi.org/10.1016/j.freeradbiomed.2014.10.581>
- Hensley, K., Gabbita, S. P., Venkova, K., Hristov, A., Johnson, M. F., Eslami, P., & Harris-White, M. E. (2013). A derivative of the brain metabolite lanthionine ketimine improves cognition and diminishes pathology in the 3 x tg-ad mouse model of Alzheimer disease. *Journal of Neuropathology & Experimental Neurology*, 72(10), 955–969. <https://doi.org/10.1097/NEN.0b013e3182a74372>
- Hensley, K., Poteskhina, A., Johnson, M. F., Eslami, P., Gabbita, S. P., Hristov, A. M., Venkova-Hristova, K. M., & Harris-White, M. E. (2016). Autophagy modulation by lanthionine ketimine ethyl ester improves long-term outcome after central fluid percussion injury in the mouse. *Journal of Neurotrauma*, 33(16), 1501–1513. <https://doi.org/10.1089/neu.2015.4196>
- Hensley, K., Venkova, K., & Christov, A. (2010b). Emerging biological importance of central nervous system lanthionines. *Molecules*, 15(8), 5581–5594. <https://doi.org/10.3390/molecules15085581>
- Hibbitts, N., Pannu, R., Wu, T. J., & Armstrong, R. C. (2009). Cuprizone demyelination of the corpus callosum in mice correlates with altered social interaction and impaired bilateral sensorimotor coordination. *ASN Neuro*, 1(3), e00013. <https://doi.org/10.1042/AN20090032>
- Hubbard, C., Benda, E., Hardin, T., Baxter, T., St, J. E., O'Brien, S., Hensley, K., & Holgado, A. M. (2013). Lanthionine ketimine ethyl ester partially rescues neurodevelopmental defects in unc-33 (dpysl2/crmp2) mutants. *Journal of Neuroscience Research*, 91(9), 1183–1190. <https://doi.org/10.1002/jnr.23239>
- Khanna, R., Wilson, S. M., Brittain, J. M., Weimer, J., Sultana, R., Butterfield, A., & Hensley, K. (2012). Opening pandora's jar: A primer on the putative roles of crmp2 in a panoply of neurodegenerative, sensory and motor neuron, and central disorders. *Future Neurology*, 7(6), 749–771. <https://doi.org/10.2217/fnl.12.68>
- Koehler, D., Shah, Z. A., Hensley, K., & Williams, F. E. (2018). Lanthionine ketimine-5-ethyl ester provides neuroprotection in a zebrafish model of okadaic acid-induced Alzheimer's disease. *Neurochemistry International*, 115, 61–68. <https://doi.org/10.1016/j.neuint.2018.02.002>
- Kornek, B., Storch, M. K., Bauer, J., Djamshidian, A., Weissert, R., Wallstroem, E., Steffler, A., Zimprich, F., Olsson, T., Lington, C., Schmidbauer, M., & Lassmann, H. (2001). Distribution of a calcium channel subunit in dystrophic axons in multiple sclerosis and experimental autoimmune encephalomyelitis. *Brain*, 124(Pt 6), 1114–1124. <https://doi.org/10.1093/brain/124.6.1114>
- Kotaka, K., Nagai, J., Hensley, K., & Ohshima, T. (2017). Lanthionine ketimine ester promotes locomotor recovery after spinal cord injury by reducing neuroinflammation and promoting axon growth. *Biochemical and Biophysical Research Communications*, 483(1), 759–764. <https://doi.org/10.1016/j.bbrc.2016.12.069>
- Lindner, M., Heine, S., Haastert, K., Garde, N., Fokuhl, J., Linsmeier, F., Grothe, C., Baumgärtner, W., & Stangel, M. (2008). Sequential myelin protein expression during remyelination reveals fast and efficient repair after central nervous system demyelination. *Neuropathology and Applied Neurobiology*, 34(1), 105–114. <https://doi.org/10.1111/j.1365-2990.2007.00879.x>
- Madadi, S., Pasbakhsh, P., Tahmasebi, F., Mortezaee, K., Khanehzad, M., Boroujeni, F. B., Noorzehi, G., & Kashani, I. R. (2019). Astrocyte ablation induced by La-aminoadipate (L-AAA) potentiates remyelination in a cuprizone demyelinating mouse model. *Metabolic Brain Disease*, 34(2), 593–603.
- Marangoni, N., Kowal, K., Deliu, Z., Hensley, K., & Feinstein, D. L. (2018). Neuroprotective and neurotrophic effects of lanthionine



- ketimine ester. *Neuroscience Letters*, 664, 28–33. <https://doi.org/10.1016/j.neulet.2017.11.018>
- Mason, J. L., Langaman, C., Morell, P., Suzuki, K., & Matsushima, G. K. (2001). Episodic demyelination and subsequent remyelination within the murine central nervous system: changes in axonal calibre. *Neuropathology and Applied Neurobiology*, 27, 50–58. <https://doi.org/10.1046/j.0305-1846.2001.00301.x>
- Matsushima, G. K., & Morell, P. (2001). The neurotoxicant, cuprizone, as a model to study demyelination and remyelination in the central nervous system. *Brain Pathology*, 11(1), 107–116. <https://doi.org/10.1111/j.1750-3639.2001.tb00385.x>
- Matute, C. (2010). Calcium dyshomeostasis in white matter pathology. *Cell Calcium*, 47(2), 150–157. <https://doi.org/10.1016/j.ceca.2009.12.004>
- Matute, C. (2011). Glutamate and atp signalling in white matter pathology. *Journal of Anatomy*, 219(1), 53–64. <https://doi.org/10.1111/j.1469-7580.2010.01339.x>
- Mimura, F., Yamagishi, S., Arimura, N., Fujitani, M., Kubo, T., Kaibuchi, K., & Yamashita, T. (2006). Myelin-associated glycoprotein inhibits microtubule assembly by a rho-kinase-dependent mechanism. *Journal of Biological Chemistry*, 281(23), 15970–15979. <https://doi.org/10.1074/jbc.M510934200>
- Moutal, A., Francois-Moutal, L., Brittain, J. M., Khanna, M., & Khanna, R. (2014). Differential neuroprotective potential of crmp2 peptide aptamers conjugated to cationic, hydrophobic, and amphipathic cell penetrating peptides. *Frontiers in Cellular Neuroscience*, 8, 471. <https://doi.org/10.3389/fncel.2014.00471>
- Moutal, A., Kalinin, S., Kowal, K., Marangoni, N., Dupree, J., Lin, S. X., Lis, K., Lisi, L., Hensley, K., Khanna, R., & Feinstein, D. L. (2019). Neuronal conditional knockout of collapsin response mediator protein 2 ameliorates disease severity in a mouse model of multiple sclerosis. *ASN neuro*, 11, 1759091419892090–1759091419892090. <https://doi.org/10.1177/1759091419892090>
- Nada, S. E., Tulsulkar, J., Raghavan, A., Hensley, K., & Shah, Z. A. (2012). A derivative of the crmp2 binding compound lanthionine ketimine provides neuroprotection in a mouse model of cerebral ischemia. *Neurochemistry International*, 61(8), 1357–1363. <https://doi.org/10.1016/j.neuint.2012.09.013>
- Nakamura, H., Takahashi-Jitsuki, A., Makiyama, H., Asano, T., Kimura, Y., Nakabayashi, J., Yamashita, N., Kawamoto, Y., Nakamura, F., Ohshima, T., Hirano, H., Tanaka, F., & Goshima, Y. (2018). Proteome and behavioral alterations in phosphorylation-deficient mutant collapsin response mediator protein2 knock-in mice. *Neurochemistry International*, 119, 207–217. <https://doi.org/10.1016/j.neuint.2018.04.009>
- Petratos, S., Ozturk, E., Azari, M. F., Kenny, R., Lee, J. Y., Magee, K. A., Harvey, A. R., McDonald, C., Taghian, K., Moussa, L., Mun, A. P., Siatskas, C., Litwak, S., Fehlings, M. G., Strittmatter, S. M., & Bernard, C. C. (2012). Limiting multiple sclerosis related axonopathy by blocking nogo receptor and crmp-2 phosphorylation. *Brain*, 135(Pt 6), 1794–1818. <https://doi.org/10.1093/brain/awr100>
- Piaton, G., Aigrot, M. S., Williams, A., Moyon, S., Tepavcevic, V., Moutkine, I., Gras, J., Matho, K. S., Schmitt, A., Soellner, H., Huber, A. B., Ravassard, P., & Lubetzki, C. (2011). Class 3 semaphorins influence oligodendrocyte precursor recruitment and remyelination in adult central nervous system. *Brain*, 134(Pt 4), 1156–1167. <https://doi.org/10.1093/brain/awr022>
- Reich, D. S., Lucchinetti, C. F., & Calabresi, P. A. (2018). Multiple sclerosis. *New England Journal of Medicine*, 378(2), 169–180. <https://doi.org/10.1056/NEJMra1401483>
- Santiago Gonzalez, D. A., Cheli, V. T., Zamora, N. N., Lama, T. N., Spreuer, V., Murphy, G. G., & Paez, P., & M. (2017). Conditional deletion of the l-type calcium channel cav1.2 in ng2-positive cells impairs remyelination in mice. *The Journal of Neuroscience*, 37(42), 10038–10051. <https://doi.org/10.1523/JNEUROSCI.1787-17.2017>
- Savchenko, V., Kalinin, S., Boullerme, A. I., Kowal, K., Lin, S. X., & Feinstein, D. L. (2019). Effects of the crmp2 activator lanthionine ketimine ethyl ester on oligodendrocyte progenitor cells. *Journal of Neuroimmunology*, 334, 576977. <https://doi.org/10.1016/j.jneuroim.2019.576977>
- Sen, M. K., Mahns, D. A., Coorsen, J. R., & Shortland, P. J. (2022). The roles of microglia and astrocytes in phagocytosis and myelination: Insights from the cuprizone model of multiple sclerosis. *Glia*, 70(7), 1215–1250.
- Shen, D., Hensley, K., & Denton, T. T. (2018). Multiple-step, one-pot synthesis of 2-substituted-3-phosphono-1-thia-4-aza-2-cyclohexene-5-carboxylates and their corresponding ethyl esters. *Bioorganic & Medicinal Chemistry Letters*, 28(4), 562–565. <https://doi.org/10.1016/j.bmcl.2018.01.052>
- Shen, K., Reichelt, M., Kyauk, R. V., Ngu, H., Shen, Y. A., Foreman, O., Modrusan, Z., Friedman, B. A., Sheng, M., & Yuen, T. J. (2021). Multiple sclerosis risk gene Mertk is required for microglial activation and subsequent remyelination. *Cell Reports*, 34(10), 108835.
- Silva, R. B. M., Greggio, S., Venturin, G. T., da Costa, J. C., Gomez, M. V., & Campos, M. M. (2018). Beneficial effects of the calcium channel blocker ctk 01512-2 in a mouse model of multiple sclerosis. *Molecular Neurobiology*, 55(12), 9307–9327. <https://doi.org/10.1007/s12035-018-1049-1>
- Skripuletz, T., Lindner, M., Kotsiari, A., Garde, N., Fokuhl, J., Linsmeier, F., Trebst, C., & Stangel, M. (2008). Cortical demyelination is prominent in the murine cuprizone model and is strain-dependent. *The American Journal of Pathology*, 172(4), 1053–1061. <https://doi.org/10.2353/ajpath.2008.070850>
- Steelman, A. J., Thompson, J. P., & Li, J. (2012). Demyelination and remyelination in anatomically distinct regions of the corpus callosum following cuprizone intoxication. *Neuroscience Research*, 72(1), 32–42. <https://doi.org/10.1016/j.neures.2011.10.002>
- Stidworthy, M. F., Genoud, S., Suter, U., Mantei, N., & Franklin, R. J. (2003). Quantifying the early stages of remyelination following cuprizone-induced demyelination. *Brain Pathology*, 13(3), 329–339. <https://doi.org/10.1111/j.1750-3639.2003.tb00032.x>
- Syed, Y. A., Abdulla, S. A., & Kotter, M. R. (2017). Studying the effects of semaphorins on oligodendrocyte lineage cells. *Methods in Molecular Biology*, 1493, 363–378. [https://doi.org/10.1007/978-1-4939-6448-2\\_26](https://doi.org/10.1007/978-1-4939-6448-2_26)
- Tahmasebi, F., Barati, S., & Kashani, I. R. (2021). Effect of CSF1R inhibitor on glial cells population and remyelination in the cuprizone model. *Neuropeptides*, 89, 102179.
- Taylor, L. C., Gilmore, W., Ting, J. P., & Matsushima, G. K. (2010). Cuprizone induces similar demyelination in male and female c57bl/6 mice and results in disruption of the estrous cycle. *Journal of Neuroscience Research*, 88(2), 391–402. <https://doi.org/10.1002/jnr.22215>
- Thomas, L., & Pasquini, L. A. (2018). Galectin-3-Mediated Glial Crosstalk Drives Oligodendrocyte Differentiation and (Re)myelination. *Front Cell Neuroscience*, 12, 297.
- Thompson, A. J., Baranzini, S. E., Geurts, J., Hemmer, B., & Ciccarelli, O. (2018). Multiple sclerosis. *The Lancet*,

- 391(10130), 1622–1636. [https://doi.org/10.1016/S0140-6736\(18\)30481-1](https://doi.org/10.1016/S0140-6736(18)30481-1)
- Togashi, K., Hasegawa, M., Nagai, J., Kotaka, K., Yazawa, A., Takahashi, M., Masukawa, D., Goshima, Y., Hensley, K., & Ohshima, T. (2020). Lanthionine ketimine ester improves outcome in an mptp-induced mouse model of Parkinson's disease via suppressions of crmp2 phosphorylation and microglial activation. *Journal of the Neurological Sciences*, *413*, 116802. <https://doi.org/10.1016/j.jns.2020.116802>
- Tokuhara, N., Namiki, K., Uesugi, M., Miyamoto, C., Ohgoh, M., Ido, K., Yoshinaga, T., Yamauchi, T., Kuromitsu, J., Kimura, S., Miyamoto, N., & Kasuya, Y. (2010). N-type calcium channel in the pathogenesis of experimental autoimmune encephalomyelitis. *Journal of Biological Chemistry*, *285*(43), 33294–33306. <https://doi.org/10.1074/jbc.M109.089805>
- Uchida, Y., Ohshima, T., Sasaki, Y., Suzuki, H., Yanai, S., Yamashita, N., Nakamura, F., Takei, K., Ihara, Y., Mikoshiba, K., Kolattukudy, P., Honnorat, J., & Goshima, Y. (2005). Semaphorin3a signalling is mediated via sequential cdk5 and gsk3beta phosphorylation of crmp2: implication of common phosphorylating mechanism underlying axon guidance and Alzheimer's disease. *Genes to Cells*, *10*(2), 165–179. <https://doi.org/10.1111/j.1365-2443.2005.00827.x>
- Vega-Riquer, J. M., Mendez-Victoriano, G., Morales-Luckie, R. A., & Gonzalez-Perez, O. (2019). Five decades of cuprizone, an updated model to replicate demyelinating diseases. *Current Neuropharmacology*, *17*(2), 129–141. <https://doi.org/10.2174/1570159X15666170717120343>
- Wallin, M. T., Culpepper, W. J., Campbell, J. D., Nelson, L. M., Langer-Gould, A., Marrie, R. A., Cutter, G. R., Kaye, W. E., Wagner, L., Tremlett, H., Buka, S. L., Dilokthornsakul, P., Topol, B., Chen, L. H., & LaRocca, N. G. (2019). The prevalence of ms in the United States: A population-based estimate using health claims data. *Neurology*, *92*(10), e1029–e1040. <https://doi.org/10.1212/WNL.0000000000007035>
- Wallström, E., Diener, P., Ljungdahl, A., Khademi, M., Nilsson, C. G., & Olsson, T. (1996). Memantine abrogates neurological deficits, but not cns inflammation, in Lewis rat experimental autoimmune encephalomyelitis. *Journal of the Neurological Sciences*, *137*(2), 89–96. [https://doi.org/10.1016/0022-510X\(95\)00339-4](https://doi.org/10.1016/0022-510X(95)00339-4)
- Wasko, N. J., Kulak, M. H., Paul, D., Nicaise, A. M., Yeung, S. T., Nichols, F. C., Khanna, K. M., Crocker, S., Pachter, J. S., & Clark, R. B. (2019). Systemic tlr2 tolerance enhances central nervous system remyelination. *Journal of Neuroinflammation*, *16*(1), 158. <https://doi.org/10.1186/s12974-019-1540-2>
- Wilson, S. M., Ki, Y. S., Yang, X. F., Park, K. D., & Khanna, R. (2014). Differential regulation of collapsin response mediator protein 2 (crmp2) phosphorylation by gsk3ss and cdk5 following traumatic brain injury. *Frontiers in Cellular Neuroscience*, *8*, 135. <https://doi.org/10.3389/fncel.2014.00135>
- Xie, M., Tobin, J. E., Budde, M. D., Chen, C. I., Trinkaus, K., Cross, A. H., McDaniel, D. P., Song, S. K., & Armstrong, R. C. (2010). Rostrocaudal analysis of corpus callosum demyelination and axon damage across disease stages refines diffusion tensor imaging correlations with pathological features. *Journal of Neuropathology & Experimental Neurology*, *69*(7), 704–716. <https://doi.org/10.1097/NEN.0b013e3181e3de90>
- Zamora, N. N., Cheli, V. T., González, S., & Paez, W. R. (2020). Deletion of voltage-gated calcium channels in astrocytes during demyelination reduces brain inflammation and promotes myelin regeneration in mice. *Journal of Neuroscience*, *40*(17), 3332–3347.